Cell Transplantation, Vol. 24, pp. 1945–1955, 2015

0963-6897/15 $90.00 + .00
DOI: http://dx.doi.org/10.3727/096368914X685276
E-ISSN 1555-3892
www.cognizantcommunication.com

Bone-Forming Capacity and Biodistribution of Bone Marrow-Derived Stromal Cells Directly Loaded Into Scaffolds: A Novel and Easy Approach for Clinical Application of Bone Regeneration

Julie Léotot,*† Angélique Lebouvier,*† Philippe Hernigou,*‡ Philippe Bierling,†§ Hélène Rouard,*†¶ and Nathalie Chevallier*†

*Université Paris-Est Créteil, Faculté de médecine, Laboratoire de "Bioingénierie Cellulaire, Tissulaire et Sanguine," Créteil, France
†Etablissement Français du Sang d'Ile-de-France, Unité d'Ingénierie et de Thérapie Cellulaire, Créteil, France
‡Service de Chirurgie Orthopédique et Traumatologique, AP-HP Hôpital Henri-Mondor, Créteil, France
§INSERM UMR955, Paris-Est University, Créteil, France
¶AP-HP Hôpital Henri-Mondor – A. Chenevier, Service Hospitalier, Créteil, France

In the context of clinical applications of bone regeneration, cell seeding into scaffolds needs to be safe and easy. Moreover, cell density also plays a crucial role in the development of efficient bone tissue engineering constructs. The aim of this study was to develop and evaluate a simple and rapid cell seeding procedure on hydroxyapatite/β-tricalcium phosphate (HA/βTCP), as well as define optimal cell density and control the biodistribution of grafted cells. To this end, human bone marrow-derived stromal cells (hBMSCs) were seeded on HA/βTCP scaffolds, and we have compared bone formation using an ectopic model. Our results demonstrated a significantly higher bone-forming capacity of hBMSCs directly loaded on HA/βTCP during surgery compared to hBMSCs preseeded for 7 days in vitro on HA/βTCP before ectopic implantation. The extent of new bone formation increases with increasing hBMSC densities quantitatively, qualitatively, and in frequency. Also, this study showed that grafted hBMSCs remained confined to the implantation site and did not spread toward other tissues, such as liver, spleen, lungs, heart, and kidneys. In conclusion, direct cell loading into a scaffold during surgery is more efficient for bone regeneration, as well as quick and safe. Therefore direct cell loading is suitable for clinical requirements and cell production control, making it a promising approach for orthopedic applications. Moreover, our results have provided evidence that the formation of a mature bone organ containing hematopoietic islets needs a sufficiently high local density of grafted hBMSCs, which should guide the optimal dose of cells for clinical use.

Key words: Bone marrow-derived stromal cell transplantation; Cell seeding; Cell density; Biodistribution; Bone tissue engineering

INTRODUCTION

Reconstruction of critical-size bone defects remains a major clinical challenge in orthopedics. Bone tissue engineering, using mesenchymal stromal cells (MSCs), provides a promising approach, which has been shown to possess a significant osteogenic potential when combined with a suitable scaffold in various animal models of bone repair (3,5–7,17). However, in spite of promising case reports on bone repair based on human MSCs (hMSCs) (25,28), preclinical data regarding cell seeding on the scaffold, cell dose, and biodistribution after transplantation remain to be solved.

Cell seeding into scaffolds is of critical importance for the generation of three-dimensional (3D) cell matrix constructs suitable for tissue regeneration. It determines the initial density and spatial distribution of seeded cells in the scaffold as well as their subsequent behaviors such as proliferation, differentiation, and migration (21,22,36). Many factors can affect the efficiency of seeding and therefore tissue regeneration, including the technique employed and the initial seeding density (2,24). Currently, cells are seeded into the scaffold primarily in vitro by static or hydrodynamic methods (14,20,22). These methods would achieve cell differentiation and extracellular matrix deposition in vitro before in vivo implantation. Nevertheless, cell quality control, like cell quantification and characterization, cannot be performed at the end of the in vitro seeding phase, which is critical for clinical application. Moreover, in vitro preseeding prolongs time of culture, which will be an additional cost for cell production as well as a delay for clinical treatment. To date, there has been no comparative study on

Received May 7, 2014; final acceptance October 21, 2014. Online prepub date: October 28, 2014.
Address correspondence to Nathalie Chevallier, Etablissement Français du Sang d'Ile-de-France, Unité d'Ingénierie et de Thérapie Cellulaire, 5 rue Gustave Eiffel, 94017 Créteil cedex, France. Tel: +33 1 56 72 21 20; Fax: +33 1 56 72 76 88; E-mail: nathalie.chevallier@efs.sante.fr

the development of a novel approach based on direct cell loading versus in vitro preseeding. In our view, a direct loading of cells into the scaffold during surgery would facilitate the clinical and regulatory requirements of these innovative tissue engineering approaches.

The initial cell seeding density is a critical factor to achieve a sufficient number of cells uniformly distributed throughout the scaffold, which is optimal for new bone formation. In prior studies, the effect of varying the cell density into scaffolds was investigated for bone, cartilage, and cardiac tissues (9,14,24,26). The effect of higher seeding densities was dependent on the tissue type as well as the culture conditions. For example, high seeding densities of chondrocytes or cardiomyocytes in agarose hydrogels or synthetic polymers, respectively, yielded better structural, mechanical, and/or functional properties (9,26). In contrast, an increasing cell seeding density did not lead to an enhancement in bone formation when scaffolds are preseeded in vitro (14). However, if the preseeding stage is short (less than few hours), increasing cell number is able to enhance bone formation but rapidly reaches a plateau (24). For a therapeutic efficiency, the cell density is crucial, since a lower-than-optimum density of grafted hMSCs will lead to poor bone formation, while a greater-than-optimum density could result in cell wastage and prolonged cell expansion times. Therefore, modes of cell seeding and cell density are likely to modulate the therapeutic impact of MSCs.

Another important aspect regarding safety and efficacy of hMSCs is the biodistribution of grafted cells postimplantation. Indeed, it is important to demonstrate that grafted hMSCs are confined to the implantation site and do not spread toward other tissues than the intended therapeutic site, which could drive to inappropriate differentiation in some organs (4). After intravenous injection, the major transient uptake site of the cells is the lungs within the first 24–48 h, followed by redistribution to the liver, kidneys, spleen, and heart (1,13). However, even if a local delivery should preferentially maintain MSCs in the site of injection, biodistribution studies are necessary to provide preclinical safety evaluation of this advanced therapy medicinal product (30,31).

This study aims to develop and evaluate a simple and rapid cell seeding procedure for hydroxyapatite/β-tricalcium phosphate (HA/βTCP) scaffolds, as well as define optimal cell density and control the biodistribution of grafted cells. To this end, the osteogenic ability of two different procedures was evaluated in an ectopic model of bone formation: i) preseeding of human bone marrow-derived stromal cells (hBMSCs) on the scaffold for 7 days in vitro before implantation versus ii) direct loading of hBMSCs into the scaffold during surgery. Then, hBMSCs were directly loaded into scaffolds at various cell densities to determine the optimal dose of cells for use. Finally, biodistribution of grafted hBMSCs was investigated at the implantation site and in five tissues (liver, spleen, lungs, kidneys, and heart), after direct loading on HA/βTCP scaffolds during subcutaneous implantation in mice for 6 weeks.

MATERIALS AND METHODS

Platelet Lysate Preparation

Human platelet lysate (hPL) was obtained from platelet apheresis collections performed at the Etablissement Français du Sang (Rungis, France). All apheresis products were biologically qualified in accordance with the French legislation. The platelet count in each product was measured automatically with an ABXpentra $60C^+$ (Horiba ABX, Montpellier, France). For homogenizing hPL preparation, five samples (three females and two males; 16 to 55 years old) were mixed to adjust the concentration at 10^9 platelets/ml, frozen at −80°C, and subsequently used to obtain hPL containing platelet-released growth factors. Remaining platelet bodies were eliminated by centrifugation at $1{,}400 \times g$.

Human Bone Marrow-Derived Stromal Cells (hBMSCs)

hBMSCs were isolated from bone marrow (BM) (4 ml) collected from the iliac crest of one patient (male, 15 years old) undergoing standard BM transplantation procedures (AP-HP Hôpital Henri Mondor, Créteil, France), after having received his informed consent. Nucleated cells from fresh BM were seeded at 2×10^5 cells/cm^2 in 225-cm^2 flasks (vWR, Fontenay-sous-Bois, France). hBMSCs were expanded in α-modified Eagle's medium (α-MEM; PAA, Les Mureaux, France) supplemented with 5% hPL, 0.5% ciprofloxacine (Bayer Pharma, Puteaux, France), and 2 IU/ml heparin (Sanofi-Aventis, Paris, France) to avoid clot formation. The cultures were maintained in a humidified atmosphere with 5% CO_2 at 37°C, and the culture medium was changed twice a week. Upon reaching 80% confluence, adherent cells were detached using 1× trypsin/EDTA (PAA) and replated at a density of 10^3 cells/cm^2 (passage 1: P1).

Flow Cytometry

The phenotype of hBMSCs (P1) was analyzed by flow cytometry. To this end, cells were stained for 15 min at room temperature (RT) with the following antibodies: anti-CD73 phycoerythrin (PE) (clone AD2), anti-CD90 fluoroisothiocyanate (FITC) (clone 5E10), anti-105 PE (clone 266), anti-CD45 FITC (clone 2D1) (all from BD Biosciences, Grenoble, France), anti-CD34 PE (clone AC136, Miltenyi Biotec, Bergjsch Gladbach, Germany), anti-HLA-DR APC (clone immu-357, Beckman Coulter), and their respective isotypes in accordance with manufacturers' instructions. Then, cells were washed in 1× Hank's buffered salt solution (PAA) and examined by a Canto™

II flow cytometer (BD Biosciences). The data were analyzed using BD FACS DIVA™ software (BD Biosciences). Positive expression was defined as fluorescence greater than 95% of that of the corresponding isotype-matched control antibodies.

Cell Differentiation

The capacity of hBMSCs to differentiate into the osteogenic, adipogenic, and chondrogenic lineages was determined by in vitro multilineage differentiation assays. For osteogenic and adipogenic differentiation, cells were seeded in six-well cell culture plates (PAA). For osteogenic differentiation, at 25% of confluence, the medium was replaced by α-MEM and 10% fetal bovine serum (FBS) (StemCell Technologies, Grenoble, France) supplemented with 50 μM L-ascorbic acid-2-phosphate, 10 mM β-glycerophosphate, and 0.1 μM dexamethasone (Sigma-Aldrich, Saint Quentin Fallavier, France). On day 21, the monolayers were fixed in 70% ethanol for 1 h at 4°C, then stained for 15 min with Alizarin red-S (Sigma-Aldrich) at RT. For adipogenic differentiation, at 80% confluence, the medium was replaced by a high-glucose medium (Invitrogen by Life Technologies, Villebon sur Yvette, France) supplemented with 10% FBS, 0.1 mM dexamethasone, 0.2 mM indomethacin, 0.01 mg/ml insulin, and 0.5 mM IBMX (Sigma-Aldrich). On day 21, the monolayers were fixed using 4% paraformaldehyde (vWR) for 5 min at RT, and then stained for 15 min with 0.3% Oil red O (Sigma-Aldrich)/60% isopropanol. Chondrogenic differentiation was performed in pellet culture using the Stempro® Chondrogenesis Differentiation Kit as described by the manufacturer (Life Technologies). On day 21, pellets were fixed in 4% formaldehyde (Sigma-Aldrich) and embedded in paraffin. Sections (3 μm) were stained with Alcian blue 8GX (Sigma-Aldrich) and counterstained with hematoxylin (Sigma-Aldrich).

Biomaterials and Cell Loading

Scaffolds of hydroxyapatite (65%)/β tricalcium phosphate (35%) (HA/βTCP), provided by Ceraver (Roissy, France), had an average porosity of 65±5% (60±5% macroporosity; 100- to 400-μm pore diameter, and 40±5% microporosity, <10 μm pore diameter) and a specific surface area of 0.8 m²/g. The granules had a diameter of 2–3 mm and weighed 8.0±1.0 mg. For the first approach (preseeding), used in our previous work, each granule of HA/βTCP was seeded with 3×10^5 hBMSCs for 3 h in a 96-well untreated cell culture plate (PAA) at 37°C (11,20). These seeded constructs were then directly placed into a 24-well untreated cell culture plate (PAA) and cultured in α-MEM 5% hPL with 5% CO_2 at 37°C for 7 days, before implantation into mice, as previously described (11,20). For the second approach (direct loading), 1×10^5, 3×10^5, 7×10^5, or 1×10^6 hBMSCs suspended in 20 μl α-MEM 5% hPL were directly deposited on each granule of HA/βTCP during subcutaneous implantation into mice, without any contact between cells and scaffold prior to implantation. Cell-free scaffolds were implanted under similar conditions and served as controls.

Animal Model and Implantation Procedures

All animal procedures were approved by the local ethics committee (approval No. 94-612) and conducted in accordance with the European Guidelines for Animal Care (Directive 2010/63/EU). Fifteen immunodeficient SCID mice (males, 7 weeks old) purchased from Charles River Laboratories (Chatillon, France) were used in this experiment, including seven mice for histological analyses and eight mice for biodistribution analyses. The mice were anesthetized with isoflurane (Abbott, Rungis, France), and six subcutaneous dorsal pockets (0.5-cm incisions) were prepared in each one. One granule of HA/βTCP was inserted into each subcutaneous pocket, either already seeded with hBMSCs since 7 days in vitro or directly loaded with hBMSCs at this stage, and the skin was closed with 5-0 sutures (Ethicon, San Lorenzo, Puerto Rico, USA). Cell-free scaffolds were implanted under similar conditions and served as controls. The animals were sacrificed with an overdose of pentobarbital (Centravet, Maisons-Alfort, France). Constructs and organs (liver, spleen, lungs, heart, and kidneys) were harvested 24 h or each week between 1 and 7 weeks after implantation procedures.

Histology

For histological analysis, constructs were excised from mice and immediately fixed in 70% ethanol. They were decalcified in 6.8% nitric acid (vWR) for various times dependent on implantation duration and rinsed in tap water before being embedded in paraffin. Three-micrometer-thick paraffin-embedded cross sections were then treated with Masson's trichrome stain, a three-color staining protocol comprising nuclear staining with hematoxylin, cytoplasmic staining with acid fuchsin/xylidine ponceau, and collagen staining with Light Green SF (all from vWR). Images were visualized by standard light microscopy and captured using UC30 Digital Color Camera and CellSens Entry software (Olympus, Rungis, France). New bone formation was analyzed and quantified using ImageJ software, and new bone density was defined as the ratio of new bone area compared with total implant area.

DNA Purification and Quantitative Real-Time Polymerase Chain Reaction (qPCR)

Scaffolds and organs were excised from mice after euthanasia. Organs were cut into small pieces and weighed (up to 10 mg for spleen and up to 25 mg for other organs), before being ground with a pestle and lysed with DNA lysis buffer (Qiagen, Courtaboeuf, France). In contrast,

scaffolds were immediately placed in DNA lysis buffer after excision and ground with a pestle. Then, total DNA was isolated using QIAamp® DNA Investigator Kit (scaffolds) or QIAmp® DNA Mini Kit (organs) as described by the manufacturer (Qiagen). The DNA obtained was detected and quantified using human TaqMan® Copy Number Reference Assay, RNase P (Applied Biosystems by Life Technologies, Saint Aubin, France) and monitored with a 7500HT Fast Real-Time PCR System (Applied Biosystems).

Statistical Analysis

Bone formation experiments were performed with hBMSCs derived from one BM donor, with $n=6$ independent experiments for each condition and quantification of three to six sections randomly distributed in each specimen. For human gDNA detection, $n=2$–4 independent experiments were realized per time for each condition, and analyses were performed in duplicate for each sample. All quantitative data were nonparametric and expressed as median and the confidence interval (CI): median ($CI_{5\%}$–$CI_{95\%}$) data were presented using boxplots. Mann–Whitney test was used for the comparisons of two groups. Comparisons between more than two groups were done with the Kruskal–Wallis test with a Dunn's multiple comparison test. The above tests were conducted using GraphPad Prism5 software. Frequency of bone formation was analyzed with chi-square test. A value of $p \leq 0.05$ was considered to be statistically significant.

RESULTS

Characterization of hBMSCs

Cell samples were used to confirm hBMSC characteristics (Fig. 1). These cells had a typical fibroblastic aspect when cultured in α-MEM supplemented with 5% hPL, as we previously described (11). Analysis of the phenotype of hBMSCs confirmed that these cells were positive for CD90, CD105, and CD73, whereas they remained negative for CD34, CD45, and HLA-DR (Fig. 1a). Culture of hBMSCs in conditioned medium for the differentiation toward osteogenic, chondrogenic, and adipogenic lineages showed that hBMSCs were able to differentiate into osteoblasts, chondrocytes, and adipocytes as demonstrated by a positive staining with, respectively, Alizarin red (Fig. 1b), Alician blue (Fig. 1c), and Oil red O (Fig. 1d).

Comparison of Bone-Forming Capacity of hBMSCs Based on Two Approaches of Cell Seeding

We have compared in vivo bone-forming capacity of hBMSCs after 7 weeks of ectopic implantation into immunodeficient SCID mice. Cells, 3×10^5, were seeded

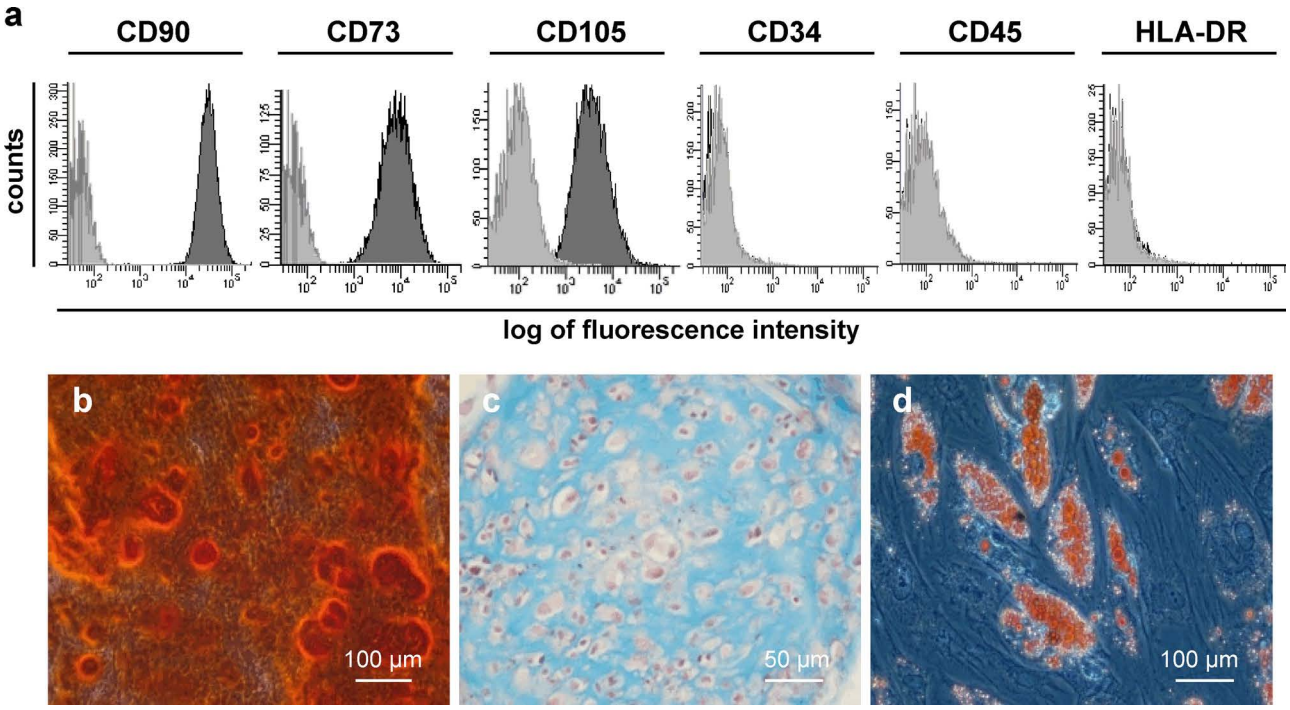

Figure 1. Phenotype and differentiation of human bone marrow-derived mesenchymal stromal cells (hBMSCs) in vitro. (a) Flow cytometry analysis for positive (CD90-FITC, CD73-PE, and CD105-PE) and negative (CD34-PE, CD45-FITC, and HLA-DR-APC) markers (black histogram) compared to their corresponding isotype (gray histogram). (b–d) Osteogenic (b), chondrogenic (c), and adipogenic (d) differentiation following Alizarin red, Alician blue, and Oil red O staining, respectively. Scale bars as indicated.

on HA/βTCP scaffolds based on two distinct approaches: i) preseeding of hBMSCs on the scaffold for 7 days in vitro before implantation or ii) direct loading of hBMSCs into the scaffold during implantation (Fig. 2). Histological analysis revealed new bone formation for all HA/βTCP preseeded for 7 days in vitro with hBMSCs, while new bone formation was observed in five of six HA/βTCP directly loaded with hBMSCs during surgery, but these frequencies were not significantly different (Fig. 2a–c). In both seeding conditions, this new bone tissue contained osteocyte-like cells and osteoblast-like cells lining the surface (Fig. 2a, b). However, BM-like elements were only observed for the direct loading condition (Fig. 2b). For scaffolds with bone formation, a quantitative analysis was performed (Fig. 2d). With direct loading, 35% of the scaffold was replaced by bone, and new bone formation was more than six times larger compared to the preseeded scaffold.

Comparison of Bone-Forming Capacity of hBMSCs Directly Loaded With Various Cell Densities

Since direct cell loading led to increased bone formation, various hBMSC doses were tested to determine the amount of cells leading to optimal bone tissue regeneration. Thus, bone-forming capacity was investigated 7 weeks postimplantation of 1×10^5, 3×10^5, 7×10^5, or 1×10^6 hBMSCs directly loaded on HA/βTCP scaffolds during surgery (Figs. 3, 4). Cell-free scaffolds were implanted under similar conditions and served as controls. New bone formation was observed only for HA/βTCP loaded with hBMSCs (Fig. 3b–e). This new tissue contained osteocyte-like cells and osteoblast-like cells lining the surface. For scaffolds with bone formation, a quantitative analysis was performed (Fig. 4a–c). Compared to total implant area, a median of 4.5% (1.4–5.5%; 10^5 hBMSCs), 30.9% (15.8–35.9%; 3×10^5 hBMSCs), 21.5% (16.0–35.5%; 7×10^5 hBMSCs), and

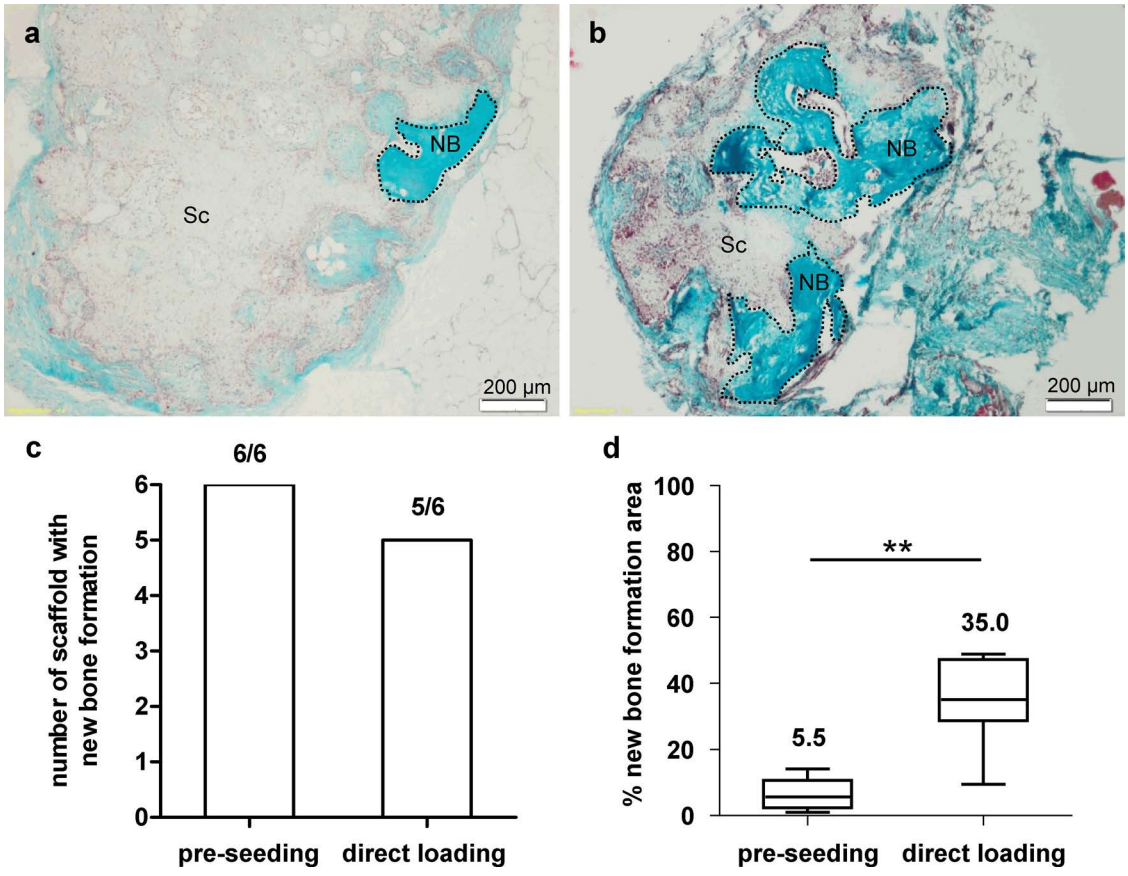

Figure 2. Comparison of in vivo bone formation after ectopic implantation of 3×10^5 hBMSCs associated with hydroxyapatite/β-tricalcium phosphate (HA/βTCP) into immunodeficient SCID mice for 7 weeks according to two distinct approaches: preseeding of hBMSCs on the scaffold for 7 days in vitro (a) versus direct loading of hBMSCs into the scaffold during surgery (b) ($n=6$ scaffolds per condition). (a, b) Histological analysis was performed after decalcification, embedding in paraffin, and Masson's trichrome staining (blue/green, collagen and bone; purple, nuclei; pink, cytoplasm). Dotted lines correspond to the areas of new bone formation. NB, new bone; Sc, scaffold. Scale bars: 200 µm. (c) Frequency of new bone formation compared to total scaffold number. (d) Quantification of new bone formation defined as the ratio of new bone area compared with total implant area. $^{**}p<0.01$.

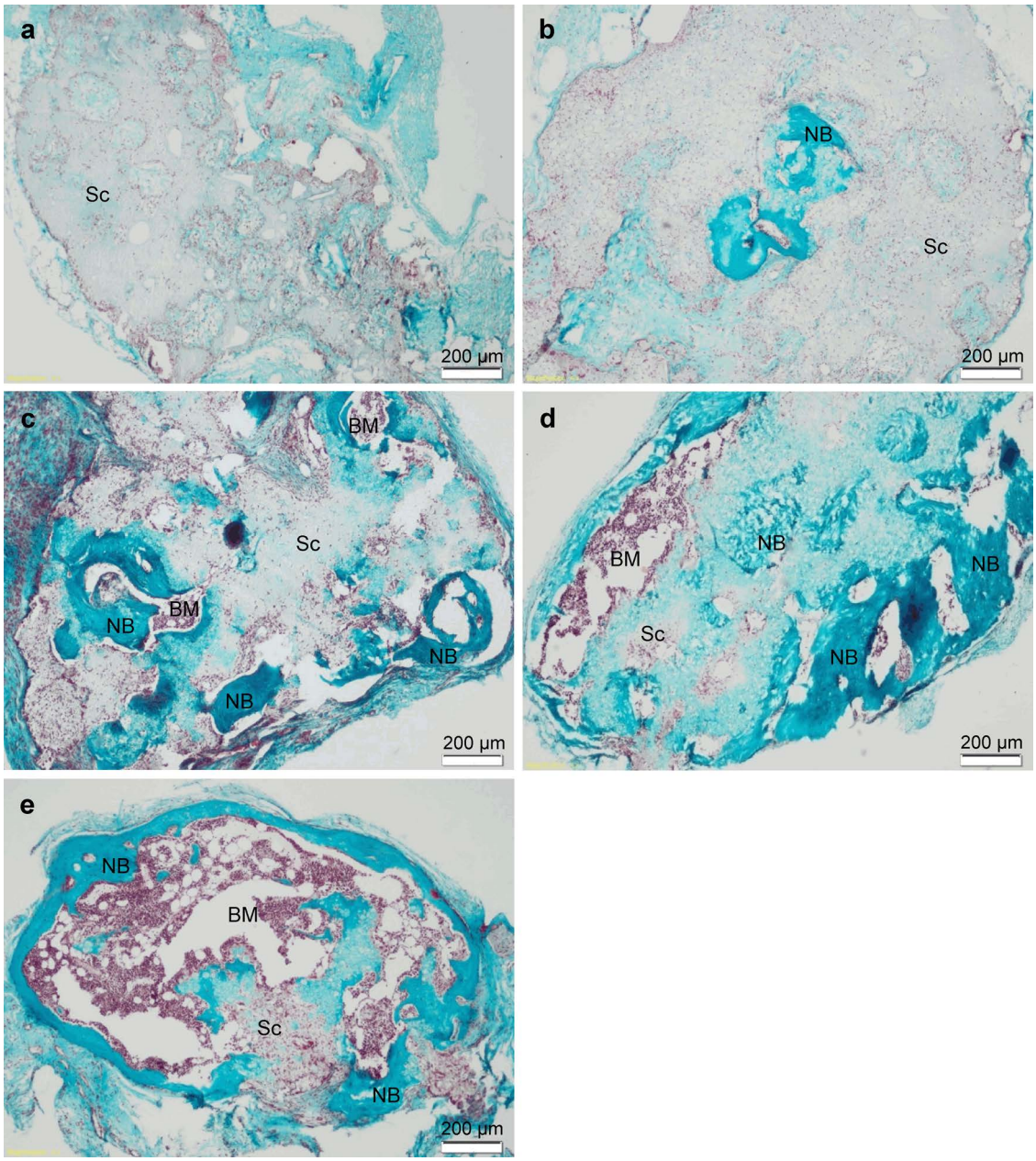

Figure 3. Histological analysis of HA/βTCP scaffolds with (b–e) or without hBMSCs (a) after ectopic implantation into immunodeficient SCID mice for 7 weeks. Scaffolds were directly loaded during surgery with 10^5 (b), 3×10^5 (c), 7×10^5 (d), and 10^6 (e) hBMSCs ($n=6$ scaffolds per condition). This analysis was performed after decalcification, embedding in paraffin, and Masson's trichrome staining (blue/green, collagen and bone; purple, nuclei; pink, cytoplasm). NB, new bone; BM, bone marrow-like elements; Sc, scaffold. Scale bars: 200 µm.

42.2% (38.5–47.3%; 10^6 hBMSCs) of new bone formation was observed (Fig. 4a). In contrast, there was no bone formation, but loosely organized connective tissues for controls (Fig. 3a). BM-like elements were also evident in association with bone formation, with a median of 0.2% (0.0–1.2%; 10^5 hBMSCs), 3.2% (1.0–7.0%; 3×10^5 hBMSCs), 4.6% (3.4–9.4%; 7×10^5 hBMSCs), and 25% (21.6–40.6%; 10^6 hBMSCs) (Figs. 3b–e, 4b). Furthermore, with the maximal cell dose (10^6 hBMSCs), scaffolds were almost totally resorbed; only 33% of the biomaterial is still present and was replaced by a mature bone, comprising bone formation and BM-like elements (Fig. 4c). A frequency analysis of new bone formation was also performed (Fig. 4d). This analysis highlighted that the increase in cell density led also to an improved bone formation rate, with a significant difference between

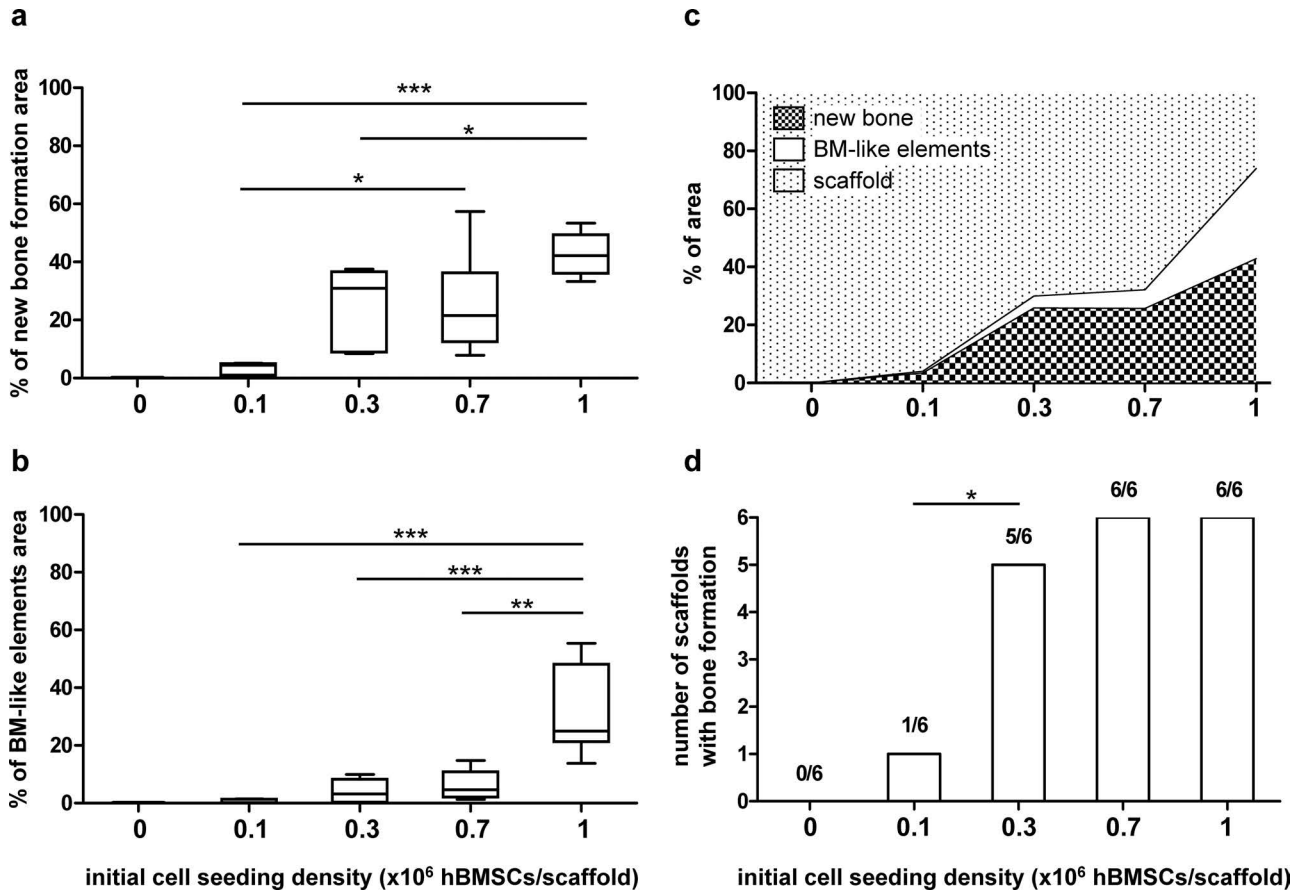

Figure 4. Analysis of in vivo new bone formation after ectopic implantation of HA/βTCP with increased hBMSC densities into immunodeficient mice for 7 weeks. Scaffolds were directly loaded with 0, 1×10^5, 3×10^5, 7×10^5, and 1×10^6 hBMSCs ($n=6$ scaffolds per condition). (a, b) Quantification of new bone formation (a) and BM-like elements (b) defined as the percentage of area compared with total implant area. (c) Quantification of mature bone (new bone, squared pattern) plus BM-like elements (white pattern) and scaffold remaining (dotted pattern), defined as the percentage of area compared with total implant area. (d) Frequency of new bone formation compared to total scaffold number. *$p<0.05$; **$p<0.01$; ***$p<0.001$.

a loading of 10^5 hBMSCs and 3×10^5 hBMSCs. No significant differences were observed with higher cell doses.

Biodistribution of Grafted hBMSCs Postimplantation

The biodistribution of grafted hBMSCs was investigated postimplantation, in both scaffolds and various organs, to control location and the possible spreading of grafted cells toward other tissues than the intended therapeutic site. For this study, we used a highly sensitive and specific assay by qPCR to detect the presence of human cells on the scaffold, as well as in the heart, spleen, lungs, liver, and kidneys, after in vivo implantation of 10^6 hBMSCs directly loaded into HA/βTCP (Table 1). Specificity of RNAse P primers was verified by the absence of PCR product when running the PCR with murine DNA as template, after implantation of cell-free scaffolds under similar conditions (controls). A standard curve was generated with serial dilutions of hBMSCs (Fig. 5). The relationship between the number of hBMSCs and the RNAse P signal was excellent, with a correlation coefficient of $r^2=0.9986$ and an efficiency of $E=99.97\%$. The detection limit was 0.41% of hBMSCs, which corresponds to 13 hBMSCs in 20 ng of DNA. Below this threshold, RNAse P signal was detected, but it was no longer quantifiable. Our results highlighted the presence of human cells on scaffolds from 24 h to 6 weeks postimplantation (Table 1). In contrast, we did not detect hBMSCs in tested organs like heart, spleen, lungs, liver, and kidneys, throughout the kinetic.

DISCUSSION

The main objective of this study was to develop and evaluate a simple and rapid cell seeding procedure for HA/βTCP scaffolds, as well as define optimal cell density and control the biodistribution of grafted cells to the intended site for clinical use. To this end, we used an ectopic model of bone formation to investigate i) cell seeding technique

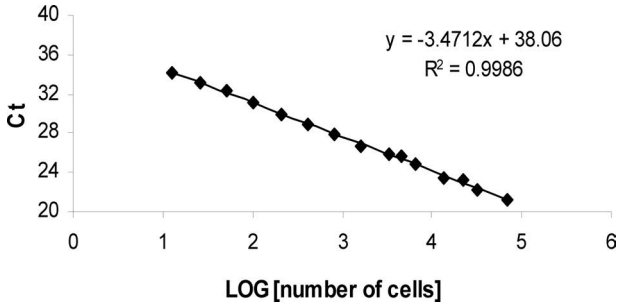

Figure 5. Standard curve of hBMSCs quantified using RNAse P signal determination by qPCR. Results are presented as copy threshold (Ct) according to logarithm (LOG) of cell number obtained following serial dilutions of human DNA.

and ii) initial seeding density. As we have previously demonstrated, hPL used as culture supplement can prime hBMSCs toward osteoblatic lineage (11). We did not use any osteoinductive agents, which is another critical point for clinical use due to safety reasons.

There is still no consensus on whether tissue-engineered bone grafts need to be cultured in vitro before implantation. Many studies have suggested that in vitro culture can allow the seeded cells to stably adhere on the scaffold and, thereby, prevent their detachment, migration, or death resulting from changes of microenvironment (22,27,35). Moreover, it would achieve cell differentiation and extracellular matrix deposition in vitro before in vivo implantation (2). Indeed, we have previously shown that preseeding of cells for 7 days in vitro on HA/βTCP did not affect cell viability and could induce osteogenic differentiation based on the expression of bone sialoprotein, osteocalcin, and osteopontin (20). Here our results demonstrated that direct hBMSC loading into scaffolds during surgery was more efficient to induce in vivo bone formation. Indeed, we showed sixfold superior osteogenic activity with a direct cell loading compared to the in vitro preseeding method. This could be due to the in vivo microenvironment that would increase the osteogenic differentiation potential of direct loaded HA/βTCP. On the other hand, we previously showed that a preseeded scaffold did not enhance sufficiently the expression of vascular endothelial growth factor to obtain a good vascularization in vivo (20). So we can make the hypothesis that the in vivo microenvironment might stimulate our cells to secrete proangiogenic factors, which would impact their survival. These results were not consistent with a study of Baba et al. who has suggested a more effective bone regeneration with preseeded hBMSCs on scaffold than injecting cultured hBMSCs into a scaffold during surgery (2). However, we did not use the same scaffold nor culture medium, and we demonstrated that both parameters can have an impact on cell behavior (11,12). Furthermore, our results showed that preseeding was not a prerequisite for cell penetration and distribution throughout the constructs since we have observed new bone formation inside the scaffold after direct hBMSCs loading.

The effect of the seeding density has been attended in a number of in vitro and in vivo studies for different cell types and biomaterials (14,21,24,26). Among them, there are several reports demonstrating that higher seeding densities do not inevitably produce better results concerning seeding efficiency, proliferation, differentiation, and tissue formation. High initial seeding densities might have negative repercussions on nutrient availability, cellular metabolism, and cell viability (15). Hence, it seems worthwhile to estimate the optimal seeding density for each cell sort and scaffold type in order to potentiate tissue engineering applications and also minimize the number of cells required and thus the in vitro cell expansion step, which is a critical point for clinical protocols. In the present study, hBMSCs of increasing densities were directly loaded on HA/βTCP during subcutaneous implantation into mice, and the amount of both bone and BM-like element (or hematopoiesis) formation was investigated in each implant after 7 weeks. Our data revealed that new bone formation increases with increasing hBMSC density in terms of frequency, quantity, and maturity. Effectively, our results showed that an increased frequency of new bone formation correlated with increasing hBMSC density, with a maximal frequency reached from 7×10^5 hBMSCs per scaffold. Nevertheless, the

Table 1. Biosdistribution of Grafted Human Bone Marrow-Derived Mesenchymal Stromal Cells (hBMSCs) Postimplantation

	Direct Loading of hBMSCs							
	24 h	1 Week	2 Weeks	3 Weeks	4 Weeks	5 Weeks	6 Weeks	Controls
Scaffolds	+	+	+	+	+	+	+	–
Lungs	–	–	–	–	–	–	–	–
Kidneys	–	–	–	–	–	–	–	–
Liver	–	–	–	–	–	–	–	–
Spleen	–	–	–	–	–	–	–	–
Heart	–	–	–	–	–	–	–	–

Human DNA detection by qPCR following direct loading of hBMSCs into HA/βTCP scaffolds, from 24 h to 6 weeks postimplantation in mice. Controls, cell-free scaffolds; (+), detection of human RNAse P gene; (–), no detection of human RNAse P gene.

dependence of bone formation on grafted cell number turned out to be far from linear. First, in scaffolds with 1×10^5 hBMSCs, bone formation was minimal. Then, new bone formation increased abruptly from 1×10^5 to 3×10^5 and from 7×10^5 to 1×10^6 hBMSCs per scaffold. Once a moderate amount of bone had been formed (around 30% of the implanted scaffold), it was accompanied by a significant development of hematopoietic islets. An increase in grafted hBMSC number from 3×10^5 to 7×10^5 cells was not linked to a corresponding rise in bone formation nor in hematopoietic elements (around 5% of implanted scaffold). In contrast, a further increase with 1×10^6 hBMSCs led to a mature bone representing more than 70% of the implanted scaffold and corresponding mainly to an increase in hematopoietic elements (30%). Taken together, our results indicated that a high cell seeding density (1×10^6 hBMSCs per 8.0 ± 1.0 mg of HA/βTCP scaffold) seemed to be a critical point to obtain the formation of a mature bone organ. We were not sure that a further increase beyond this dose would lead to a better bone formation. Indeed, Friedenstein's group showed that when pieces of mouse femoral marrow had been transplanted under the renal capsule, increases in the size of grafted tissue failed to yield proportional increases in the size of the mature implants (18). The authors suggested that when the numbers of grafted cells exceed the capacity of transplantation site, a fraction of them forms a surplus, or a reserve, of bone-forming cells. Besides, in our study, the presence of hematopoiesis in only some implants could be explained by the fact that hematopoiesis only occurs when a significant amount of bone has formed and only when this bone is sizable enough to encapsulate a hematopoietic space. This assumption was supported by data of Mankani et al. (24) who established that the formation of a mature bone organ, including the presence of hematopoiesis, requires a sufficiently high local density of bone, which in turn requires a sufficient number of grafted hBMSCs. This can be attributed to the direct and indirect action of grafted hMSCs that are able to differentiate into tissue-specific cells and/or act on host cells by secreting soluble factors, which promote cell migration, proliferation, and differentiation and also support hematopoiesis (8,23). Furthermore, the scaffold resorption rate was related to the amount of new bone formation, and cell-free scaffolds did not resorb. These results indicate a good balance between new bone formation and resorption, making these HA/βTCP scaffolds suitable for clinical use.

Some studies described heterogeneity in bone-forming potential of BMSCs and donor variability. For example, Tortelli et al. suggested that origin and type of bone formation were strictly dependent on the nature and commitment of grafted cells (33). Besides, Janicki et al. described a negative correlation to donor age: hBMSCs capable of forming bone were derived from significantly younger donors (16). In the present study, using bone-competent hBMSCs from a young BM donor, our results clearly indicated that a direct cell loading was more efficient than preseeding. These data suggested that the potential of the cells was also dependent on the manner of grafting them, which was also highlighted by other studies comparing various scaffolds (12). By taking into account all the variation causing the heterogeneity, and because to date there does not exist a reliable marker to identify bone-competent cells, we cannot pretend to give the exact number of cells that would be needed to obtain bone formation for all patients (16,19). Nevertheless, our results showed that a high number of bone-competent cells is a prerequisite to obtain a good induction of bone formation. It would be very important now to define the phenotype of bone-competent cells in order to be able to treat patients with the highest efficacy.

An important safety consideration for tissue engineering approaches is the biodistribution of grafted cells, with a need to define their potential of trafficking, homing, engraftment, differentiation, and persistence in both target and nontarget tissues. Biodistribution will be impacted by the route of administration, with an intravenously administered product having a very different distribution potential to a product in which cells are adhered to scaffolds or locally injected into a specific tissue (32). While the lungs were the major uptake site after intravenous injection, in models with local injection, grafted cells remained for a long time at the injection site. For example, after intramuscular injection, no human DNA was detected in any evaluated tissues outside muscle (29). In contrast, after intra-articular injection, human Alu sequences were found in heart, spleen, intestine, brain, blood, or testis, but this detection was very low and uncommon as it was found only in 10% to 20% of analyzed mice (34). In the present study, our data demonstrated that after direct loading, grafted hBMSCs remained at the implantation site, on scaffolds, from 24 h to 6 weeks postimplantation. This indicated that grafted cells were able to survive up to 6 weeks postimplantation, as was also suggested by others (10,33). Furthermore, grafted hBMSCs did not have unwanted homing as no human cells were detected throughout the kinetic, in tissues such as lungs, liver, spleen, kidneys, and heart. These results confirmed that grafted hBMSCs remained on HA/βTCP and provided evidence of the absence of spreading of these cells toward the other tissues. In our previous work, we have demonstrated a good adhesion and distribution of hBMSCs on HA/βTCP scaffolds by scanning electron microscopy as soon as 3 h after seeding (20). Taken together, these data indicate a good cell attachment to these scaffolds and a particular tropism of hBMSCs for the biomaterial,

even without any contact between cells and scaffold prior to implantation.

In summary, we have established that direct cell loading into a scaffold during surgery is more efficient for bone regeneration, as well as quick, safe, useful, and suitable for clinical requirements, making it a promising approach for orthopedic applications. Moreover, our results have provided evidence that the formation of both hematopoiesis and a mature bone organ need a sufficient high local density of hBMSCs, which should guide the optimal dose of cells for clinical use.

ACKNOWLEDGMENTS: This work was supported by the Etablissement Français du Sang d'Ile-de-France, the Université Paris-Est Créteil and has received funding from the European Union's Seventh Programme for research, technological development and demonstration under grant agreement No. 241879. J. Léotot was supported by the DIM-STEM-Pôle Ile-de-France. We would like to thank Dr. M. Gervais-Taurel for her help on statistical analyses. We also thank the Centre de Recherches Chirurgicales Dominique Chopin for the use of their animal platform facilities. We are grateful to the company Ceraver, which kindly provided the ceramics. The authors declare no conflicts of interest.

REFERENCES

1. Allers, C.; Sierralta, W. D.; Neubauer, S.; Rivera, F.; Minguell, J. J.; Conget, P. A. Dynamic of distribution of human bone marrow-derived mesenchymal stem cells after transplantation into adult unconditioned mice. Transplantation 78(4):503–508; 2004.
2. Baba, S.; Inoue, T.; Hashimoto, Y.; Kimura, D.; Ueda, M.; Sakai, K.; Matsumoto, N.; Hiwa, C.; Adachi, T.; Hojo, M. Effectiveness of scaffolds with pre-seeded mesenchymal stem cells in bone regeneration--Assessment of osteogenic ability of scaffolds implanted under the periosteum of the cranial bone of rats. Dent. Mater. J. 29(6):673–681; 2010.
3. Boo, J. S.; Yamada, Y.; Okazaki, Y.; Hibino, Y.; Okada, K.; Hata, K.; Yoshikawa, T.; Sugiura, Y.; Ueda, M. Tissue-engineered bone using mesenchymal stem cells and a biodegradable scaffold. J. Craniofac. Surg. 13(2):231–239; discussion 240–243; 2002.
4. Breitbach, M.; Bostani, T.; Roell, W.; Xia, Y.; Dewald, O.; Nygren, J. M.; Fries, J. W.; Tiemann, K.; Bohlen, H.; Hescheler, J.; Welz, A.; Bloch, W.; Jacobsen, S. E.; Fleischmann, B. K. Potential risks of bone marrow cell transplantation into infarcted hearts. Blood 110(4):1362–1369; 2007.
5. Bruder, S. P.; Kraus, K. H.; Goldberg, V. M.; Kadiyala, S. The effect of implants loaded with autologous mesenchymal stem cells on the healing of canine segmental bone defects. J. Bone Joint Surg. Am. 80(7):985–996; 1998.
6. Cancedda, R.; Dozin, B.; Giannoni, P.; Quarto, R. Tissue engineering and cell therapy of cartilage and bone. Matrix Biol. 22(1):81–91; 2003.
7. Caplan, A. I. Review: Mesenchymal stem cells: Cell-based reconstructive therapy in orthopedics. Tissue Eng. 11(7–8): 1198–1211; 2005.
8. Caplan, A. I.; Dennis, J. E. Mesenchymal stem cells as trophic mediators. J. Cell. Biochem. 98(5):1076–1084; 2006.
9. Carrier, R. L.; Papadaki, M.; Rupnick, M.; Schoen, F. J.; Bursac, N.; Langer, R.; Freed, L. E.; Vunjak-Novakovic, G. Cardiac tissue engineering: Cell seeding, cultivation parameters, and tissue construct characterization. Biotechnol. Bioeng. 64(5):580–589; 1999.
10. Chai, Y. C.; Roberts, S. J.; Desmet, E.; Kerckhofs, G.; van Gastel, N.; Geris, L.; Carmeliet, G.; Schrooten, J.; Luyten, F. P. Mechanisms of ectopic bone formation by human osteoprogenitor cells on CaP biomaterial carriers. Biomaterials 33(11):3127–3142; 2012.
11. Chevallier, N.; Anagnostou, F.; Zilber, S.; Bodivit, G.; Maurin, S.; Barrault, A.; Bierling, P.; Hernigou, P.; Layrolle, P.; Rouard, H. Osteoblastic differentiation of human mesenchymal stem cells with platelet lysate. Biomaterials 31(2):270–278; 2010.
12. Coquelin, L.; Fialaire-Legendre, A.; Roux, S.; Poignard, A.; Bierling, P.; Hernigou, P.; Chevallier, N.; Rouard, H. In vivo and in vitro comparison of three different allografts vitalized with human mesenchymal stromal cells. Tissue Eng. Part A 18(17–18):1921–1931; 2012.
13. Detante, O.; Moisan, A.; Dimastromatteo, J.; Richard, M. J.; Riou, L.; Grillon, E.; Barbier, E.; Desruet, M. D.; De Fraipont, F.; Segebarth, C.; Jaillard, A.; Hommel, M.; Ghezzi, C.; Remy, C. Intravenous administration of 99mTc-HMPAO-labeled human mesenchymal stem cells after stroke: In vivo imaging and biodistribution. Cell Transplant. 18(12):1369–1379; 2009.
14. Grayson, W. L.; Bhumiratana, S.; Cannizzaro, C.; Chao, P. H.; Lennon, D. P.; Caplan, A. I.; Vunjak-Novakovic, G. Effects of initial seeding density and fluid perfusion rate on formation of tissue-engineered bone. Tissue Eng. Part A 14(11):1809–1820; 2008.
15. Issa, R. I.; Engebretson, B.; Rustom, L.; McFetridge, P. S.; Sikavitsas, V. I. The effect of cell seeding density on the cellular and mechanical properties of a mechanostimulated tissue-engineered tendon. Tissue Eng. Part A 17(11–12):1479–1487; 2011.
16. Janicki, P.; Boeuf, S.; Steck, E.; Egermann, M.; Kasten, P.; Richter, W. Prediction of in vivo bone forming potency of bone marrow-derived human mesenchymal stem cells. Eur. Cell Mater. 21:488–507; 2011.
17. Kon, E.; Muraglia, A.; Corsi, A.; Bianco, P.; Marcacci, M.; Martin, I.; Boyde, A.; Ruspantini, I.; Chistolini, P.; Rocca, M.; Giardino, R.; Cancedda, R.; Quarto, R. Autologous bone marrow stromal cells loaded onto porous hydroxyapatite ceramic accelerate bone repair in critical-size defects of sheep long bones. J. Biomed. Mater. Res. 49(3):328–337; 2000.
18. Kuralesova, A. I.; Leontovich, A. M.; Krukovets, I. L.; Fridenshtein, A. [Quantitative characteristics of the transfer of the hematopoietic microenvironment]. Biull. Eksp. Biol. Med. 98(12):739–741; 1984.
19. Larsen, K. H.; Frederiksen, C. M.; Burns, J. S.; Abdallah, B. M.; Kassem, M. Identifying a molecular phenotype for bone marrow stromal cells with in vivo bone-forming capacity. J. Bone Miner. Res. 25(4):796–808; 2010.
20. Leotot, J.; Coquelin, L.; Bodivit, G.; Bierling, P.; Hernigou, P.; Rouard, H.; Chevallier, N. Platelet lysate coating on scaffolds directly and indirectly enhances cell migration, improving bone and blood vessel formation. Acta Biomater. 9(5):6630–6640; 2013.
21. Lode, A.; Bernhardt, A.; Gelinsky, M. Cultivation of human bone marrow stromal cells on three-dimensional scaffolds of mineralized collagen: Influence of seeding density on

colonization, proliferation and osteogenic differentiation. J. Tissue Eng. Regen. Med. 2(7):400–407; 2008.
22. Luo, F.; Hou, T. Y.; Zhang, Z. H.; Xie, Z.; Wu, X. H.; Xu, J. Z. Effects of initial cell density and hydrodynamic culture on osteogenic activity of tissue-engineered bone grafts. PLoS One 8(1):e53697; 2013.
23. Majumdar, M. K.; Thiede, M. A.; Haynesworth, S. E.; Bruder, S. P.; Gerson, S. L. Human marrow-derived mesenchymal stem cells (MSCs) express hematopoietic cytokines and support long-term hematopoiesis when differentiated toward stromal and osteogenic lineages. J. Hematother. Stem Cell Res. 9(6):841–848; 2000.
24. Mankani, M. H.; Kuznetsov, S. A.; Robey, P. G. Formation of hematopoietic territories and bone by transplanted human bone marrow stromal cells requires a critical cell density. Exp. Hematol. 35(6):995–1004; 2007.
25. Marcacci, M.; Kon, E.; Moukhachev, V.; Lavroukov, A.; Kutepov, S.; Quarto, R.; Mastrogiacomo, M.; Cancedda, R. Stem cells associated with macroporous bioceramics for long bone repair: 6- to 7-year outcome of a pilot clinical study. Tissue Eng. 13(5):947–955; 2007.
26. Mauck, R. L.; Seyhan, S. L.; Ateshian, G. A.; Hung, C. T. Influence of seeding density and dynamic deformational loading on the developing structure/function relationships of chondrocyte-seeded agarose hydrogels. Ann. Biomed. Eng. 30(8):1046–1056; 2002.
27. Ouyang, A.; Yang, S. T. Effects of mixing intensity on cell seeding and proliferation in three-dimensional fibrous matrices. Biotechnol. Bioeng. 96(2):371–380; 2007.
28. Quarto, R.; Mastrogiacomo, M.; Cancedda, R.; Kutepov, S. M.; Mukhachev, V.; Lavroukov, A.; Kon, E.; Marcacci, M. Repair of large bone defects with the use of autologous bone marrow stromal cells. N. Engl. J. Med. 344(5):385–386; 2001.
29. Ramot, Y.; Meiron, M.; Toren, A.; Steiner, M.; Nyska, A. Safety and biodistribution profile of placental-derived mesenchymal stromal cells (PLX-PAD) following intramuscular delivery. Toxicol. Pathol. 37(5):606–616; 2009.
30. Sensebe, L.; Fleury-Cappellesso, S. Biodistribution of mesenchymal stem/stromal cells in a preclinical setting. Stem Cells Int. 2013:678063; 2013.
31. Sharpe, M. E.; Morton, D.; Rossi, A. Nonclinical safety strategies for stem cell therapies. Toxicol. Appl. Pharmacol. 262(3):223–231; 2012.
32. Tolar, J.; O'Shaughnessy, M. J.; Panoskaltsis-Mortari, A.; McElmurry, R. T.; Bell, S.; Riddle, M.; McIvor, R. S.; Yant, S. R.; Kay, M. A.; Krause, D.; Verfaillie, C. M.; Blazar, B.R. Host factors that impact the biodistribution and persistence of multipotent adult progenitor cells. Blood 107(10):4182–4188; 2006.
33. Tortelli, F.; Tasso, R.; Loiacono, F.; Cancedda, R. The development of tissue-engineered bone of different origin through endochondral and intramembranous ossification following the implantation of mesenchymal stem cells and osteoblasts in a murine model. Biomaterials 31(2):242–249; 2010.
34. Toupet, K.; Maumus, M.; Peyrafitte, J. A.; Bourin, P.; van Lent, P. L.; Ferreira, R.; Orsetti, B.; Pirot, N.; Casteilla, L.; Jorgensen, C.; Noël, D. Long-term detection of human adipose-derived mesenchymal stem cells after intraarticular injection in SCID mice. Arthritis Rheum. 65(7):1786–1794; 2013.
35. Zhang, Z. Y.; Teoh, S. H.; Chong, W. S.; Foo, T. T.; Chng, Y. C.; Choolani, M.; Chan, J. A biaxial rotating bioreactor for the culture of fetal mesenchymal stem cells for bone tissue engineering. Biomaterials 30(14):2694–2704; 2009.
36. Zhou, H.; Weir, M. D.; Xu, H. H. Effect of cell seeding density on proliferation and osteodifferentiation of umbilical cord stem cells on calcium phosphate cement-fiber scaffold. Tissue Eng. Part A 17(21–22):2603–2613; 2011.